

Unification scheme of radio galaxies and quasars falsified by their observed size distributions

Ashok K. Singal and Raj Laxmi Singh

*Astronomy and Astrophysics Division, Physical Research Laboratory,
Navrangpura, Ahmedabad - 380 009, India*

asingal@prl.res.in

ABSTRACT

In the currently popular orientation-based unified scheme, a radio galaxy appears as a quasar when its principal radio-axis happens to be oriented within a certain cone opening angle around the observer's line of sight. Due to geometrical projection, the observed sizes of quasars should therefore appear smaller than those of radio galaxies. We show that this simple, unambiguous prediction of the unified scheme is not borne out by the actually observed angular sizes of radio galaxies and quasars. Except in the original 3CR sample, based on which the unified scheme was proposed, in other much larger samples no statistically significant difference is apparent in the size distributions of radio galaxies and quasars. The population of low-excitation radio galaxies with apparently no hidden quasars inside, which might explain the observed excess number of radio galaxies at low redshifts, cannot still account for the absence of any foreshortening of the sizes of quasars at large redshifts. On the other hand from infrared and X-ray studies there is evidence of hidden quasar within a dusty torus in many RGs, at $z > 0.5$. It seems difficult how to reconcile this with the absence of foreshortening of quasar sizes at even these redshifts, and perhaps one has to allow that the major radio axis may not have anything to do with the optical axis of the torus. Otherwise to resolve the dichotomy of radio galaxies and quasars, a scheme quite different from the present might be required.

Subject headings: galaxies: active — quasars: general — galaxies: nuclei — radio continuum: general

1. Introduction

The observed numbers and radio sizes of quasars both appear to be about a factor of two smaller than those of radio galaxies (RGs), in the radio strong 3CR complete sample (Laing et al. 1983), in the redshift range $0.5 < z < 1$ (Barthel 1989). It was suggested that both RGs and quasars belong to the same parent population of radio sources, and that a source appears as

a quasar only when its principal radio-axis happens to be oriented within a certain cone opening angle (ξ_c) around the observer’s line of sight (Barthel 1989). In this model, the nuclear continuum and broad-line optical emission region is surrounded by an optically-thick torus and ξ_c is the half cone-opening angle of the torus, similar to as proposed in the case of Seyfert galaxies (Antonucci & Miller 1985). In the case of RGs the observer’s line of sight is supposed to be passing through the obscured region which hides the bright optical nucleus and the broad-line region. Accordingly, RGs and quasars are considered to be intrinsically indistinguishable and all differences in their observed radio properties are attributed to their supposedly different orientations with respect to the observer’s line of sight; in particular, the observed smaller value of radio sizes of quasars in the 3CR sample was attributed to their larger geometric projection effects because of the shallower inclinations of their radio axes with respect to the observer’s line of sight.

This has come to be known as orientation-based unified scheme (OUS) and has gained increasing popularity (Antonucci 1993; Antonucci 2012; Urry & Padovani 1995; Kembhavi & Narlikar 1999) both because of its simplicity and the promise it holds to bring two apparently quite distinct class of objects, viz. quasars and RGs, under one roof. According to this scheme, the expected ratios of the observed numbers as well as of sizes of quasars and RGs in a low-frequency radio-complete sample are determined purely by the value of ξ_c . It is widely believed that, in samples picked at metre wavelengths, the observed number as well as sizes of quasars are typically about half as large as those of RGs. This notion has resulted purely from the data in a limited redshift range ($0.5 < z < 1$) of the 3CR sample that yielded the ‘canonical’ value of $\xi_c \sim 45^\circ$. Later Singal (1993a) pointed out that the data in other redshift bins from the rest of the 3CR sample do not seem to fit into this simple scenario. Suggestions were then put forward (Gopal-Krishna et al. 1996) that by making allowance for a temporal evolution of sources in both size and luminosity, one could mitigate the above discrepancy. Alternatively it has been suggested that this excess may be due to a population of low-excitation radio galaxies (LERGs), which might make a significant contribution to the number of FR II-type radio galaxies at low redshifts (see e.g. Hine & Longair 1979). Laing et al. (1994) have pointed out that these optically dull LERGs are unlikely to appear as quasars when seen end-on and that these should be excluded from the sample while testing the unified scheme models. From Infra-red observations also there is evidence of a population of powerful radio galaxies, concentrated at low redshifts, which lack the hidden quasar (Antonucci 2012; Ogle et al. 2006; Leipski et al. 2010). Using both X-ray and Mid-IR data, Hardcastle et al. (2009) showed conclusively that almost all objects classed as LERGs in optical spectroscopic studies lack a radiatively efficient active nucleus. On the other hand strong evidence against OUS comes also from the observed opposite behaviour of the luminosity–size correlations among RGs and quasars as well as from the vast difference in their cosmological size evolutions (Singal 1988, 1993b, 1996a).

A comparison of the angular size of RGs and quasars is a very robust test, as in samples selected at metre wavelengths, emission only from the steep spectrum extended parts of the source is observed, with flat-spectrum core-emission, if any, highly suppressed and the relativistic beaming effects playing almost no part. Both quasars and RGs are picked by the strength of their extended

emission, not affected by any orientation effects. As the parent sample for RGs and quasars is supposed to be the same, there will be no relative selection effects based on redshift or luminosity, with their observed size ratios affected only by the geometrical projection. Further, it is not necessary to convert their angular sizes into linear sizes (using a particular cosmological model) for the comparison of their sizes to test OUS as the observed angular size ratios will truly reflect their (projected) linear size ratios since the redshift distribution is supposed to be the same for RGs and quasars in OUS models. If we think that the redshift distribution might be different for RGs and quasars, then we are already doubting the veracity of the unified scheme.

2. The Source Sample

For our investigations we have chosen an essentially complete MRC sample (Kapahi et al. 1998a,b), which is about a factor ~ 5 deeper than the 3CR sample and has the required radio and optical information. It comprises a total of 550 sources, with 105 of them being quasars, six BL Lac objects, and the remainder RGs. Optical identifications for the latter are complete up to a red magnitude of ~ 24 or a K magnitude of ~ 19 . Spectroscopic redshift data are available for 60 percent of the galaxies, the remainder are mostly faint galaxies (McCarthy et al. 1996) expected to be at high redshifts $z \gtrsim 1$. Optical spectroscopic data for quasars with full observational details are given in Baker et al. (1999), with tabulations of redshifts, continuum, and emission-line data for each source. The optical identifications are missing only for a very small percent of sources (Kapahi et al. 1998a), which should not be too detrimental for our investigations here.

As only the powerful RGs are supposed to partake in unification with quasars, we have confined ourselves to only the strong, FR II-type sources (Fanaroff & Riley 1974) with $P_{408} \geq 5 \times 10^{25} \text{ W Hz}^{-1}$ (for a Hubble constant $H_0 = 71 \text{ km s}^{-1} \text{ Mpc}^{-1}$, the matter energy density $\Omega_m = 0.27$, and the vacuum energy (dark energy!) density $\Omega_\Lambda = 0.73$; Spergel et al. 2003); the quasars in any case (all but one) fall above this luminosity limit. This limit corresponds to the FR I/II luminosity break $P_{178} = 2 \times 10^{25} \text{ W Hz}^{-1} \text{ sr}^{-1}$ (for $H_0 = 50 \text{ km s}^{-1} \text{ Mpc}^{-1}$) of Fanaroff & Riley (1974). It may be prudent to exclude flat-spectrum sources entirely, since these mostly are core-dominant cases where the relativistic beaming might introduce serious selection effects. Among the quasars there are 16 sources with spectral index $\alpha \leq 0.5$ (with $S \propto \nu^{-\alpha}$), while among the RGs there are only 7 such cases; we have excluded all these flat-spectrum cases. Also there is a large fraction of Compact Steep Spectrum Sources (CSSS; linear size $< 25 \text{ kpc}$) in the MRC sample, comprising about 20 percent of the whole sample, which seem to be a different class than the FRII class of sources whose unification is sought in OUS (Kapahi et al. 1995), and as such these should be excluded for testing OUS. For the unknown- z galaxies we have taken $< 3 \text{ arcsec}$ as the CSSS criteria as at $z \sim 1$, where most of these faint galaxies are likely to be, for our adopted cosmological parameters, 1 arcsec translates to about 8 kpc .

It has been pointed out (Kapahi et al. 1995) that radio sizes of MRC quasar appear considerably larger than those of 3CR quasars. Such can of course be taken only as an indicator of

some anomaly, as the flux-density range and the volumes sampled in the two samples (MRC and 3CR) are very different. For a meaningful comparison of the relative sizes of RGs and quasars, in order to test OUS, one must draw both kind of sources (RGs and quasars) from a common parent sample, so that no effects enter due to different flux-density and/or the space-volume sampled as any redshift or luminosity dependence of the sizes could otherwise bias the conclusions. Earlier it could not be done because data on the MRC sample of galaxies were then not complete (Kapahi et al. 1995), but these data having since become available, we could now attempt it here.

There are a total of 494 sources in our sample listed in Table 2, which is organized in the following manner: (1) Source name from MRC. (2) Flux-density S_{408} at 408 MHz. (3) Spectral index α ($S \propto \nu^{-\alpha}$). (4) Nature of optical object; G: galaxy; Q: quasar; U: unidentified. (5) Redshift z , whenever a measured value is available. (6) Largest angular size θ (in arcsec). (7) Linear size l in kilo-pc. (8) Luminosity P_{408} in W/Hz. Among these 494 sources, there are 379 RGs, 87 quasars, and 28 remain unidentified. The linear size is calculated from the observed angular size θ as $l = \theta \mathcal{D} / (1 + z)$ and the luminosity is calculated from $P_{408} = 4\pi S_{408} \mathcal{D}^2 (1 + z)^{1+\alpha}$, where \mathcal{D} is the comoving cosmological distance calculated from the cosmological redshift z of the source. In general it is not possible to express \mathcal{D} in terms of z in a close-form analytical expression and one may have to evaluate it numerically. For example, in the flat universe models ($\Omega_m + \Omega_\Lambda = 1, \Omega_\Lambda \neq 0$), \mathcal{D} is given by (see e.g., Weinberg 2008),

$$\mathcal{D} = \frac{c}{H_0} \int_1^{1+z} \frac{dz}{(\Omega_\Lambda + \Omega_m z^3)^{1/2}}. \quad (1)$$

For a given Ω_Λ , \mathcal{D} can be evaluated from Eq. (1) by a numerical integration.

3. Results and Discussion

Figure 1 shows the redshift distribution of RGs and Quasars in our sample. We notice a large excess of RGs at low redshifts ($z \lesssim 0.5$), similar to the excess seen in the 3CR sample, as pointed out by Singal (1993a). Figure 2 shows the luminosity distribution of RGs and Quasars. Again we notice an excess of RGs at lower end of the FR II luminosities ($P \lesssim 10^{27}$ W Hz⁻¹). Of course we expect the luminosity distribution to largely mimic the redshift distribution because of the Malmquist bias in a flux-limited sample like the MRC. It also needs to be noted that the unknown- z RGs in the MRC sample will mostly fall at high ends of redshift and luminosity; in any case we are already finding a rather surplus number of RGs at low redshifts and luminosities than that expected from OUS.

As mentioned earlier LERGs, a population of FR II RGs with no hidden quasars, concentrated only at low redshifts (say, $z < 0.5$) could make the apparently anomalous number and size distribution of RGs and quasars at low redshifts in the 3CR sample (Singal 1993a) somewhat consistent with OUS, and perhaps it might also hold true for the MRC sample. For that more than half of the total source population at these redshifts will have to be LERGs. Another implication will

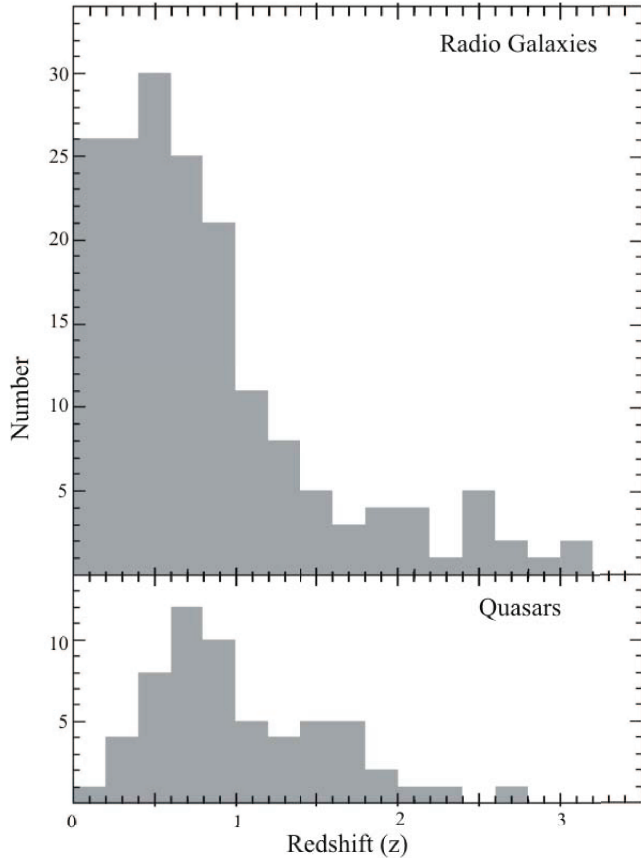


Fig. 1.— Histograms of the redshift distributions of RGs and quasars for the MRC sample.

be that LERGs, if they do indeed form an isotropic sample (as suggested by Laing et al. 1994), should show smaller projected sizes as compared with those of high-excitation radio galaxies, which supposedly lie preferentially in the sky plane. There is some evidence for that (Hardcastle et al. 1998). But could such a population of LERGs be also present in the low frequency samples at higher redshifts? For one thing such a scenario would imply that a large majority of FR II radio galaxies ($\sim 50 - 60\%$) remain a separate class (with intrinsically different properties from quasars/BLRGs) and not fall within the scope of OUS. At the same time it is also clear that if such a high percentage of LERGs is making up the low frequency samples like the 3CR at higher redshifts $z \gtrsim 0.5$ as well, then the number and size ratios, used by Barthel in his original 3CR sample in the redshift range $0.5 < z < 1$ to propose OUS, will totally go haywire and the proposition of OUS will have to be abandoned in the first place there itself.

Due to geometrical projection, the observed sizes of quasars should appear smaller than those

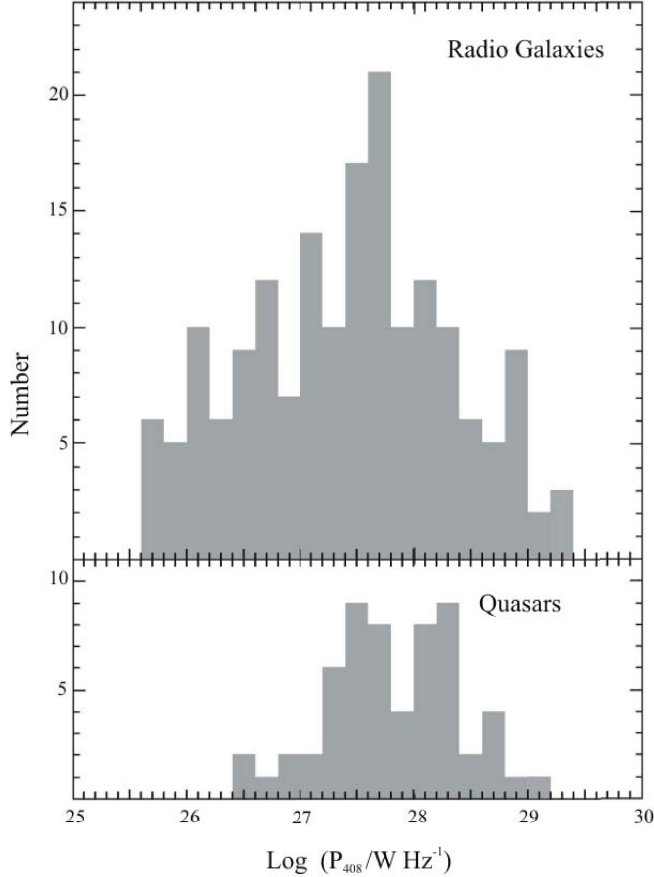


Fig. 2.— Histograms of the luminosity distributions of RGs and quasars for the MRC sample.

of radio galaxies. This is a simple, unambiguous prediction of the unified scheme which is thus falsifiable from a comparison of the observed angular sizes of radio galaxies and quasars. We therefore examine OUS by this robust test of the relative size distributions of RGs and quasars. Figure 3a shows normalized cumulative plots of angular size distribution of RGs and quasars for our chosen MRC sample, while for a comparison Figure 3b show the same for the 3CR sources. In the 3CR sample, as expected, the quasar sizes seem smaller than those of the RGs which of course was the prime basis for the OUS hypothesis. However in a much larger independent MRC sample, there seems no evidence that the quasar sizes are in any way smaller than those of RGs. Here we had retained the CSS sources and we notice a bump (discontinuity!) at or around 2 arcsec in the MRC size distributions both for RGs and quasars, due to these CSS Sources. But in figure 4, we have excluded all the CSSS cases and we see that the inclusion or exclusion of CSSS in either case does not alter any of our conclusions.

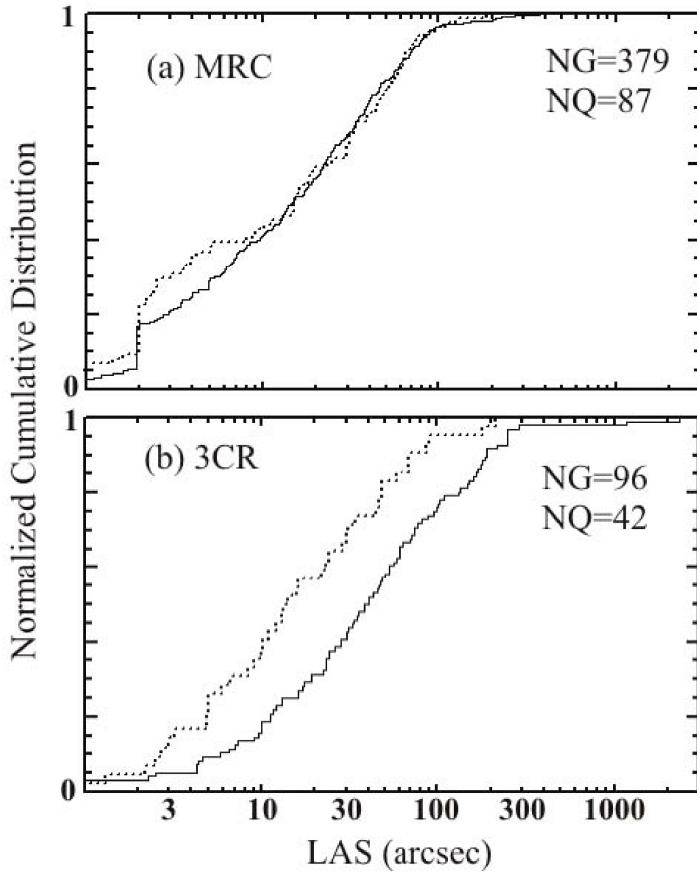


Fig. 3.— Normalized cumulative distributions of largest angular size (LAS) of RGs (continuous curves) and quasars (broken curves) (a) for the MRC sample (b) for the 3CR sample. NG and NQ give the number of RGs and quasars respectively, in each plot.

Since the two samples (MRC and 3CR) have different flux-density limits, it may be interesting to see if the difference between the two samples in the size distributions is in any way related to the flux-density level of the samples. Figure 5 shows the normalized cumulative distribution of radio sizes of RGs and quasars for the MRC sample in three different flux-density bins. To avoid any selection bias, we have chosen the flux-density bins such that there are about equal number of sources in each bin. We see no change in the earlier picture, the quasar and RGs do not show any systematic difference in their size distributions. With its basic tenet, that the observed quasar sizes should be smaller than of RGs, having been precluded, OUS is thus almost ruled out.

We should clarify that the evidence against the unification of extended RGs and quasars here does not necessarily invalidate the relativistic beaming models (Orr & Browne 1982) of the unification of core-dominated and lobe-dominated quasars. In the same way, any evidence seen

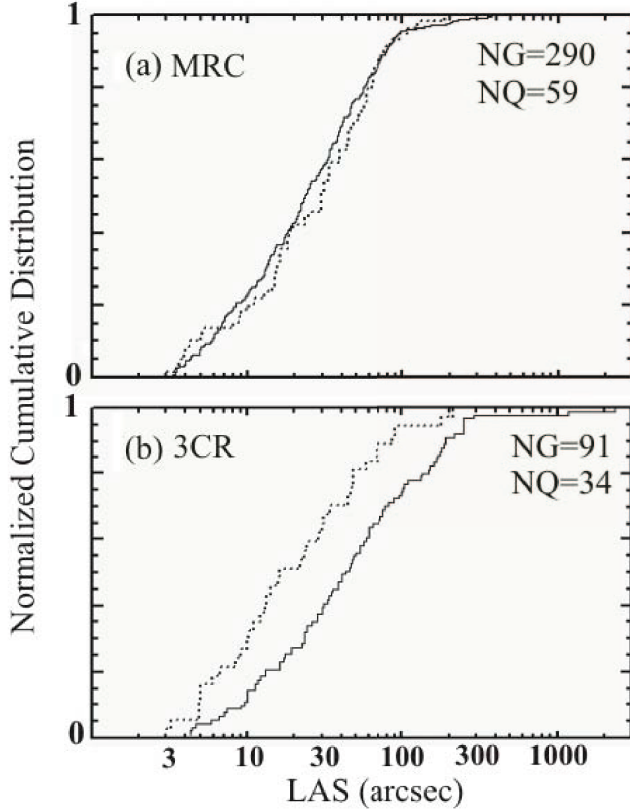


Fig. 4.— Same as Figure 3, but with CSSS excluded.

in favour of the relativistic beaming models cannot be cited in favour of unification of extended RGs and quasars. The two unifications are independent even if these have been combined in the so-called grand unification scheme models of the active galactic nuclei (Antonucci 1993; Antonucci 2012; Urry & Padovani 1995; Kembhavi & Narlikar 1999). It is quite likely that radio-loud quasars do not make a randomly oriented population; the question here is that do RGs and quasars fit together, as proposed by Barthel (1989), into one unified scheme model like OUS?

We compare in Figure 6 the size distributions of MRC sources in three different redshift bins. Again we find no evidence for quasars being smaller in size in any of the three redshift bins. As we have 116 RGs without redshift determination, and most of these will be at $z \gtrsim 1$, in Figure 7a we include these along with 46 RGs with $z \geq 1$ to compare the angular sizes of all these high redshift RGs with those of quasars at $z \geq 1$. We find that the size distributions are strikingly similar. There are also 28 unidentified cases, which again most likely will be RGs at $z \gtrsim 1$. After dropping 9 CSSS cases among them, we compare in Figure 7b the size distribution of 19 unidentified cases with that of quasars with $z \geq 1$. The two size distributions statistically look almost indistinguishable.

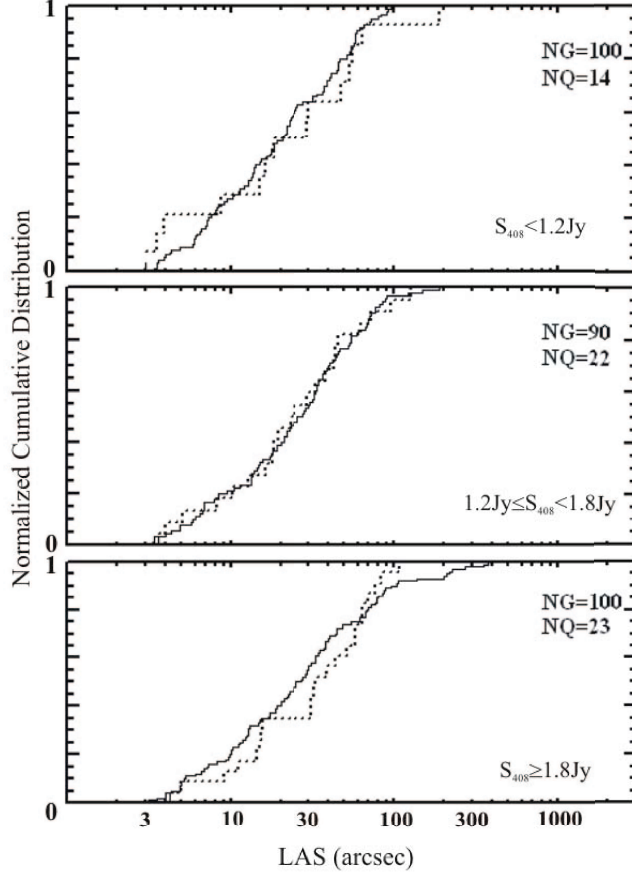


Fig. 5.— Normalized cumulative distribution of radio sizes of RGs (continuous curves) and quasars (broken curves) for the MRC sample in different flux-density bins.

We have determined median value θ_{med} (in arcsec) of the cumulative size-distribution of the source in the various sub-samples (Table 1). To get an idea of the spread around the median values we have also listed in Table 1 the lower quartiles θ_{lq} and upper quartiles θ_{uq} in all cases. We find that while in the 3CR sample quasar sizes may be half those of RGs, in the much larger MRC sample the roles seems to have been reversed (cf. Table 1) with quasars appearing to be in fact somewhat larger in size than RGs (in the whole MRC sample by a factor of ~ 1.3 though in a sub-sample like $z \geq 1$ by as much as a factor of two); in any case nowhere is there an evidence of the quasar sizes being smaller than of RGs. This is apparent not only from median values of size but also from the lower and upper quartile values in their cumulative plots.

The cone opening angle (ξ_c) consistent with the smaller quasar fraction seen in MRC data (Figures 4, 5 and 6; Table 1) will mean a value narrower than $\sim 45^\circ$ derived from the 3CR data,

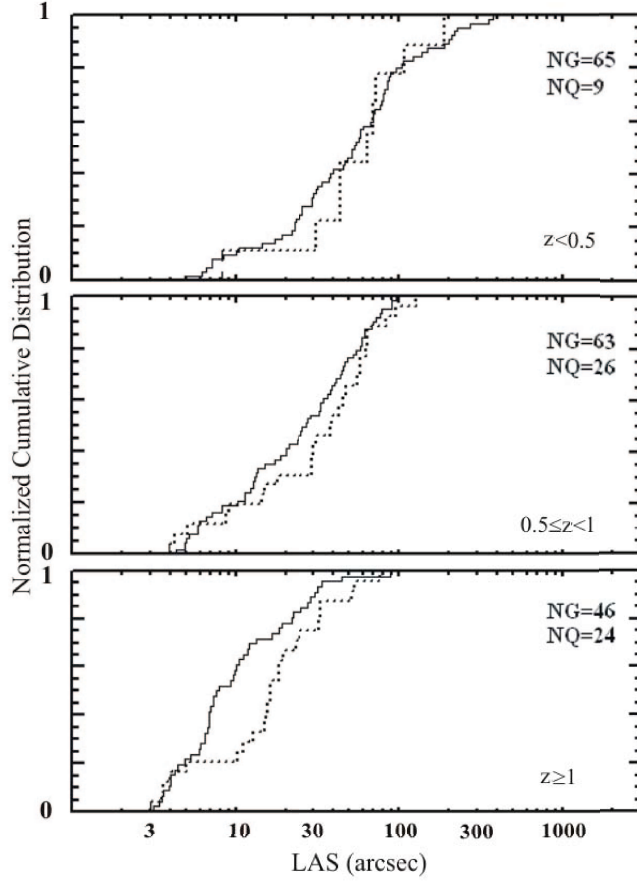


Fig. 6.— Normalized cumulative distribution of radio sizes of RGs (continuous curves) and quasars (broken curves) for the MRC sample in three different redshift ranges.

implying expected size ratio to be even more pronounced than that in the 3CR case. After dropping CSS sources, in the MRC sample the fraction of quasars is $59/(290 + 59) \sim 0.17$, implying only about one sixth of the sources are quasars (as compared to one third in 3CR sample of Barthel (1989), based on which OUS, with a cone opening angle $\xi_c \sim 45^\circ$, was proposed). That such a low fraction of quasars is in itself an evidence against the popular OUS scheme was already pointed out by Singal (1996b). In a picture consistent with OUS, MRC quasar sizes should be statistically smaller than of RGs by more than a factor of two, but we on the other hand find quasars to be rather somewhat bigger in size (by a factor of ~ 1.3) than even of RGs, which could never happen in an OUS type of scheme. Thus there is no consistency at all in the number count ratios and the size ratios and no cone opening angle (ξ_c) can be found within OUS that would satisfy both relative number counts and relative size distributions observed for both quasars and RGs. Thus

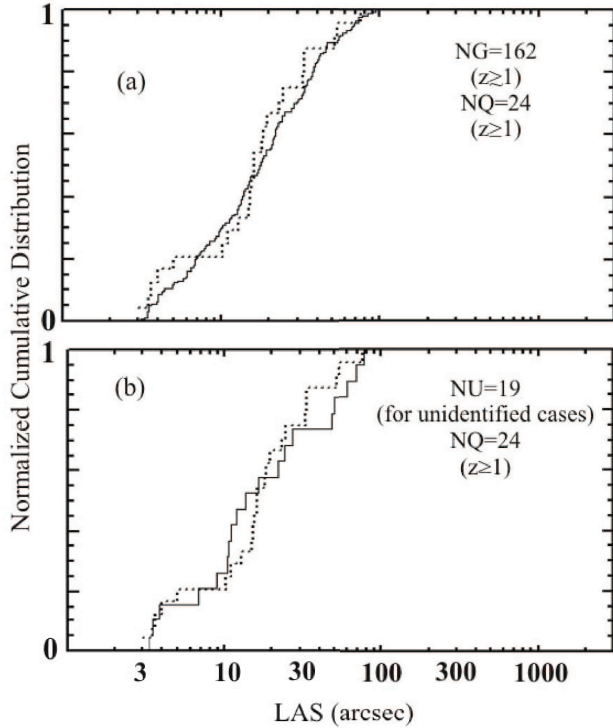


Fig. 7.— Normalized cumulative distribution of radio sizes of (a) RGs (continuous curves) comprising 46 sources with $z \geq 1$ and 116 unknown-redshift galaxies (a total of 162 RGs with expected $z \gtrsim 1$), and quasars (broken curves) for $z \geq 1$ and (b) unidentified sources (continuous curves) and quasars (broken curves) for $z \geq 1$.

the predictions of OUS are not corroborated by the data in a sample other than the 3CR at even high redshift bins $z > 0.5$ (and at high luminosities), where LERGs may not play an important part, and OUS is clearly ousted in that sense.

It is clear that at a few Jy or weaker levels, OUS does not hold good. If we still want to hold on to OUS, in the belief that it might be valid at or above only the higher flux levels of 3CR radio sources ($S_{408} > 4$ Jy), then since the integrated source counts fall rapidly with flux ($N(> S) \propto S^{-1}$), it is only a tiny fraction of the RGs that would be taking part in the currently popular OUS. In fact one would then be proposing a division of RGs into further sub-classes (beyond LERGs seen only at low redshifts and low luminosities within FR II types RGs), out of which perhaps only one minor sub-class of RGs will be partaking in OUS, thus sounding more like a further *disunification scheme* for RGs. And even there it will have to be one of those “cosmic conspiracies” where two or more sub-classes of RGs of apparently very different size distributions manage to get their combined

Table 1: Median and quartile values of size distributions for RGs and quasars.

Sub-sample	NG	θ_{lq}	θ_{med}	θ_{uq}	NQ	θ_{lq}	θ_{med}	θ_{uq}
All 3CR	91	17	40	98	34	10	18	45
All MRC	290	11	22	46	59	14	30	54
$S_{408} < 1.2$	100	9	21	42	14	8	24	50
$1.2 \leq S_{408} < 1.8$	90	14	26	45	22	12	24	44
$S_{408} \geq 1.8$	100	12	27	55	23	15	33	60
$z < 0.5$	65	25	54	86	9	38	64	91
$0.5 \leq z < 1$	63	11	27	38	26	15	39	58
$z \geq 1$	46	6	8	17	24	11	16	24

size-distribution very similar to that of quasars in all flux-density and redshift bins.

By still adhering to the belief that may be a restricted class of RGs partakes in the OUS model, it seems that much effort is being put on giving perhaps rather undue weight to a small select sub-sample ($0.5 < z < 1$ redshift bin of 3CR) that happened to be the first one to get examined in this regard. Except for that particular bin of the 3CR sample, which incidentally was instrumental in the proposition of the unified scheme with the “canonical” value $\xi_c \sim 45^\circ$, other samples do not seem to yield the expected size ratios, in fact as we saw there seems to be no statistically significant difference in the size distribution of quasars and RGs.

At the same time infrared and X-ray studies do find many cases of obscured hidden quasar in powerful radio galaxies, implying that a unified scheme must be true to some extent. Most 3CR FRII radio galaxies with $0.5 \lesssim z < 1$ do show strong, quasar-like mid-IR emission (Antonucci 2012), while at $z \lesssim 0.5$ there is suggestion of a dearth of hidden AGN in FRII RGs. For example, Meisenheimer et al (2001) observed at infrared wavelengths 10 quasars and 10 RGs, selected with matched luminosity and the redshift distributions from the 3CR catalogue, and found the results compatible with hidden Quasars, except possibly for some at the low luminosity/redshift end. Shi et al (2005) used the Spitzer photometry to study a sample of 3CR radio galaxies and the behavior of the sources is consistent with the presence of an obscuring circumnuclear torus. The X-ray spectroscopic survey of 38 high- z 3CR objects of Wilkes et al (2009) is extremely supportive of complete unification of 3CR radio galaxies and Quasars at $z \gtrsim 1$. It seems rather quizzical how to reconcile such overwhelming evidence for torus with the equally strong evidence for the lack of foreshortening of radio sizes of quasar at all redshifts.

The predictions of the unified scheme models are not corroborated by the radio observations

and that seems to refute the presently popular OUS. At the same time it does not seem likely that, except perhaps in some very contrived scenario, any modification of OUS, such as an evolutionary model of ξ_c with redshift or luminosity, could yield quasar sizes comparable to those of galaxies in all bins, since in OUS those will be expected to be smaller due to geometrical projection everywhere. On the other hand quasar sizes are not found to be smaller than those of galaxies for any of the bins, whether in flux-density or in redshift, in the MRC sample. Perhaps we may have to allow that the orientation of the extended radio structure does not relate to the axis of the torus, which amounts to abandoning a basic tenet of OUS, or we may require some very different unification scheme than the currently popular orientation-based unified scheme model.

4. Conclusion

We showed that contrary to the expectations in OUS models, observed quasar sizes are not in any way systematically smaller than those of galaxies. The absence of this foreshortening of the sizes of quasars as compared to those of RGs of similar flux densities or at similar redshifts, provides irrefutable evidence against the unified scheme models. To still uphold OUS, one would need to propose FR II type RGs with no hidden quasars, and/or of small intrinsic radio sizes at *all* redshifts and luminosities, i.e., across the entire gamut of population of strong radio galaxies, with a large majority of RGs opting out of OUS. It means first one would rather require a robust *disunification scheme* of the radio galaxies themselves before an attempt could be made to unify a rather small number of RGs with quasars in a scheme like OUS. Or perhaps one has to allow that the major radio axis does not coincide with the axis of the torus, which is a basic tenet of the present unification scheme. In any case it appears that the dichotomy of RGs and quasars among extragalactic radio sources cannot be resolved within the present frame-work of OUS, which therefore seems falsified.

REFERENCES

- Antonucci, R. 1993, ARA&A, 31, 473
- Antonucci, R. 2012, arXiv:1101.0837
- Antonucci, R. R. J., & Miller, J. S. 1985, ApJ, 297, 621
- Baker, J. C., Hunstead, R. W., Kapahi, V. K., & Subrahmanya, C. R. 1999, ApJS, 122, 29
- Barthel, P. D. 1989, ApJ, 336, 606
- Fanaroff, B. L., & Riley, J. M. 1974, MNRAS, 167, 31P
- Gopal-Krishna, Kulkarni V. K., & Wiita, P. J. 1996, ApJ, 463, L1
- Hardcastle, M. J., Alexander, P., Pooley, G. G., & Riley, J. M. 1998, MNRAS, 296, 445
- Hardcastle, M. J., Evans, D. A., & Croston, J. H. 2009, MNRAS, 396, 1929
- Hine R. G., Longair M. S. 1979, MNRAS, 188, 111
- Kapahi, V. K., et al. 1995, JAAS, 16, 125
- Kapahi, V. K., Athreya, R. M., van Breugel, W., McCarthy, P. J., & Subrahmanya, C. R. 1998a, ApJS, 118, 275
- Kapahi, V. K., et al. 1998b, ApJS, 118, 327
- Kemhavi, A. K. & Narlikar, J. V. 1999, Quasars and Active Galactic Nuclei - An Introduction, Cambridge University, Cambridge, p. 357
- Laing, R. A., Riley, J. M., & Longair, M. S. 1983, MNRAS, 204, 151
- Laing R. A., Jenkins C. R., Wall J. V., Unger S. W. 1994, in Bicknell V., Dopita M. A., Quinn P. J., eds, ASP Conf. Ser. Vol. 54, The First Stromlo Symposium: The Physics of Active Galaxies. ASP, San Francisco, p. 201
- Leipski, C., et al. 2010, ApJ, 717, 766
- McCarthy, P. J., Kapahi, V. K., van Breugel, W., Persson, S. E., Athreya, R. M., & Subrahmanya, C. R. 1996, ApJS, 107, 19
- Meisenheimer, K., Haas, M., Müller, S. A. H., Chini, R., Klaas, U., & Lemke, D. 2001, A&A, 372, 719
- Ogle, P., Whysong, D., & Antonucci, R. 2006, ApJ 647, 161
- Orr, M. J. L., & Browne, I. W. A. 1982, MNRAS, 200, 1067

- Shi, Y., et al. 2005, ApJ, 629, 88
- Singal A. K. 1988, MNRAS, 233, 87
- Singal A. K. 1993a, MNRAS, 262, L27
- Singal A. K. 1993b, MNRAS, 263, 139
- Singal A. K. 1996a, in R. Ekers et al., eds, IAU Symp. 175, Extragalactic Radio Sources. D. Ridel, Dordrecht, p. 563
- Singal A. K. 1996b, MNRAS, 278, 1069
- Spergel, D. N., et al. 2003, ApJS, 148, 175
- Urry, C. M., & Padovani, P. 1995, PASP, 107, 803
- Weinberg, S. 2008, Cosmology, Oxford University, Oxford, p. 43
- Wilkes, B., et al. 2009, in Wolk, S., Fruscione, A. & Swartz, D., eds, Chandra’s First Decade of Discovery, Proc. conf., Boston, MA, abstract 206

Table 2:: Radio and optical data for our sample.

Source Name (1)	S_{408} Jy (2)	α (3)	Opt Obj (4)	z (5)	θ " (6)	l kpc (7)	P_{408} W Hz ⁻¹ (8)
B0001-237	1.77	0.83	G	0.315	33.8	155	5E26
B0006-212	1.18	0.73	G	0.91	0.9	7	4E27
B0007-287	1.13	0.87	U		68.3		
B0015-229	1.11	1.16	G	2.01	10.5	89	4E28
B0017-205	1.96	0.78	G	0.197	372	1202	2E26
B0017-207	1.25	0.95	Q	0.545	96	612	1E27
B0020-253	5.36	0.78	G	0.35	79	388	2E27
B0022-297	7.83	0.87	Q	0.406	44	238	4E27
B0023-203	3.43	0.95	G	0.845	8.1	62	1E28
B0023-263	17	0.64	G	0.322	1.9	9	5E27
B0025-204	1.03	0.77	G		11.1		
B0025-277	1.29	0.92	G		13.7		
B0028-223	1.18	0.79	G	0.205	23.2	77	1E26
B0029-232	1.09	1.07	G		21.9		
B0029-243	1.96	1.15	G	1.29	4	34	2E28
B0029-271	1.21	0.96	Q	0.333	1	5	4E26
B0030-219	1.08	1.06	G	2.168	0.9	8	4E28
B0030-220	1.01	0.93	Q	0.806	3.9	29	3E27
B0030-297	1.63	1.02	G		1.9		
B0032-203	6.87	1.08	G	0.516	1.5	9	7E27
B0034-234	1.69	1.11	G		15.6		
B0035-231	1.21	0.99	G	0.685	2.3	16	2E27
B0037-258	1.21	0.96	G	1.1	27.6	227	8E27
B0038-294	1.01	0.87	G		17.5		
B0040-208	1.12	0.9	Q	0.657	2	14	2E27
B0041-224	1.85	1.23	G		45		
B0042-248	1.45	0.87	G		73		
B0050-222	1.41	0.98	G	0.654	1.9	13	3E27
B0052-241	1.18	1.14	G	2.86	2.5	20	1E29
B0055-256	1.18	0.97	G	0.199	22.8	74	1E26

Table 2 – *continued*

Source Name (1)	S_{408} Jy (2)	α (3)	Opt Obj (4)	z (5)	θ " (6)	l kpc (7)	P_{408} W Hz ⁻¹ (8)
B0055-258	1.02	1.13	G		58		
B0056-242	1.88	0.98	G		73		
B0058-229	1.24	0.95	Q	0.706	63	452	3E27
B0100-277	3.01	0.96	G		67		
B0101-275	1.86	1.06	G		1.9		
B0102-256	1.95	1.07	G		0.9		
B0103-243	1.15	0.96	G		20.8		
B0106-233	1.13	0.85	Q	0.818	2.5	19	3E27
B0106-291	3.41	0.92	G		1.9		
B0110-224	1.31	1.05	G		3.4		
B0111-256	0.98	0.68	Q	1.05	2.2	18	5E27
B0112-209	2.2	1.14	G		38.1		
B0112-219	0.98		U				
B0113-245	1.38	0.83	U		50		
B0113-285	1.69	0.77	G		9.5		
B0114-211	10.64	0.87	G	1.41	1.9	16	1E29
B0115-261	2.58	0.74	G	0.268	10	41	5E26
B0121-295	1.46	0.96	G		30.1		
B0122-255	3.76	0.93	U		48.1		
B0123-226	1.54	0.58	Q	0.717	5.1	37	3E27
B0125-201	1.08	0.89	G		1.9		
B0125-216	1.29	0.81	G	0.34	25.5	123	5E26
B0127-276	1.02	0.77	G	0.318	1.9	9	3E26
B0128-264	5.36	1.2	G		33.4		
B0133-266	1.19	0.97	Q	1.53	53.5	458	2E28
B0133-277	0.97	1.03	G		40.3		
B0136-231	1.3	0.54	Q	1.895	12.8	109	2E28
B0137-263	1.46	0.83	G	0.16	77	210	1E26
B0138-218	0.96	0.97	G		20.6		
B0139-273	5.04	1.02	G	1.44	11.7	100	7E28

Table 2 – *continued*

Source Name (1)	S_{408} Jy (2)	α (3)	Opt Obj (4)	z (5)	θ " (6)	l kpc (7)	P_{408} W Hz ⁻¹ (8)
B0140-257	1	1.24	G	2.64	3.4	28	8E28
B0143-246	1.51	0.86	G	0.716	52.5	379	3E27
B0144-227	1.18	0.81	G	0.6	1.9	13	2E27
B0146-224	1.65	0.81	G	0.36	14.3	72	7E26
B0147-288	1.28	0.95	G		3.3		
B0148-297	7.04	0.82	G	0.41	138	749	4E27
B0149-260	1.05	0.95	G	0.144	96.5	241	6E25
B0149-299	2.42	0.83	G	0.603	17.1	115	3E27
B0150-275	1.94	0.91	G		4		
B0152-209	1.55	1.11	G	1.89	1	9	4E28
B0152-260	1.31	0.87	G		37		
B0155-212	2.39	1.04	G	0.159	86	234	2E26
B0155-225	1.4	0.95	G		37.6		
B0156-252	1.39	1.04	G	2.09	6.8	57	5E28
B0156-278	0.96	0.76	G	0.33	5	24	3E26
B0201-214	1.28	0.85	G	0.915	1.9	15	5E27
B0203-209	1.1	1.09	G	1.257	12	101	1E28
B0205-223	0.96	0.99	G		24.2		
B0205-229	1.77	0.83	G	0.68	34.4	243	3E27
B0208-240	1.87	0.74	G	0.23	67	244	3E26
B0209-237	1.5	0.92	Q	0.68	18	127	3E27
B0222-224	2.36	0.95	Q	0.23	2.4	9	4E26
B0222-234	5.44	0.79	Q	1.617	15.5	133	8E28
B0246-231	2.44	0.7	Q	2.904	0.99	8	1E29
B0209-282	1.56	0.81	G	0.6	13.3	89	2E27
B0211-256	1.07	1.05	G	1.3	2.4	20	1E28
B0211-258	1.19	0.82	G		46		
B0216-250	4.14	0.98	G		55.2		
B0221-285	3.86	1.08	G		14.5		
B0223-245	1.03	0.75	G	0.634	0.9	6	2E27

Table 2 – *continued*

Source Name (1)	S_{408} Jy (2)	α (3)	Opt Obj (4)	z (5)	θ " (6)	l kpc (7)	P_{408} W Hz ⁻¹ (8)
B0225-241	2.16	0.78	G	0.52	5.2	32	2E27
B0226-284	1.063	0.69	G	0.21	58	197	1E26
B0226-292	1.12	0.97	G		1.9		
B0230-245	2.1	0.93	G	0.88	11.3	88	8E27
B0231-235	4.09	1.02	G	0.81	38.4	290	1E28
B0233-290	1.96	1	G	0.725	4.9	36	5E27
B0237-201	1.5	0.85	G	1.03	19.1	155	8E27
B0242-221	0.98	1.12	G		1.9		
B0245-263	0.97	0.76	G	0.35	6.2	30	4E26
B0245-297	1.16	0.75	G	0.36	57	285	5E26
B0246-202	1.69	0.8	G	0.58	1.9	12	2E27
B0247-205	1.12	1.53	G	0.32	2.9	13	4E26
B0247-207	3.3	0.97	G	0.085	200	315	6E25
B0251-273	0.98	1.06	G	3.16	3.9	30	1E29
B0252-246	1.38	1.07	G	1.3	33.6	284	1E28
B0253-206	3.19	0.86	G	0.69	96	683	6E27
B0253-259	1.55	0.99	G		1.9		
B0254-236	5.87	1.1	G	0.509	33.4	205	6E27
B0254-263	1.93	1	G	0.31	6.5	29	6E26
B0254-274	1.01	1.19	G	0.48	37.4	223	9E26
B0255-247	0.97	1.09	U		1.5		
B0255-262	1.33	1.12	G	0.36	8.4	42	6E26
B0256-236	2.19	0.9	U		27.2		
B0259-252	1.14	0.98	U		22		
B0259-252	1.11	0.83	U		11		
B0305-226	4.95	0.88	G	0.268	88	359	1E27
B0305-246	1.21	1.07	G	1.265	6.4	54	1E28
B0309-260	0.95	1.41	G		15		
B0312-271	1.42	1.09	U		1.9		
B0313-271	1.82	1.14	G	0.216	227	789	2E26

Table 2 – *continued*

Source Name (1)	S_{408} Jy (2)	α (3)	Opt Obj (4)	z (5)	θ " (6)	l kpc (7)	P_{408} W Hz $^{-1}$ (8)
B0315-205	1.23	1.23	G		21.1		
B0315-282	1	0.52	Q	1.17	2	17	5E27
B0316-257	1.54	1.12	G	3.13	6.7	52	2E29
B0319-298	3.72	0.6	G	0.583	1.9	13	4E27
B0320-263	1.52	0.79	G		22.5		
B0320-267	1.15	0.68	G	0.9	4.3	34	4E27
B0324-228	1.98	1.19	G	1.89	9.6	82	6E28
B0325-260	1.04	0.74	G	0.638	59	405	2E27
B0326-288	4.03	0.83	G	0.108	17	33	1E26
B0327-261	1.57	1.3	U		60		
B0328-272	1.06	0.87	Q	1.803	18.1	155	2E28
B0337-216	1.51	0.84	G	0.414	1.1	6	9E26
B0344-291	2.14	0.72	G	0.137	4.9	12	1E26
B0345-206	1.13	0.98	G		22.5		
B0346-297	1.72	0.88	G	0.413	122	665	1E27
B0346-298	1.01	0.96	G		84		
B0349-211	1.14	0.92	G	2.31	7.2	60	4E28
B0349-278	13.7	0.73	G	0.066	350	438	1E26
B0350-279	1.24	1.15	G	1.9	1.2	10	4E28
B0353-207	1.02	0.78	U		1.9		
B0354-263	1.2	0.85	G		12.6		
B0357-247	2.16	0.87	G	0.205	30.3	101	3E26
B0357-264	1.5	0.54	U		1.9		
B0400-247	1.17	0.97	G	1.105	45.1	371	8E27
B0406-244	2.92	1.35	G	2.44	7.3	60	2E29
B0407-226	1.24	1.01	Q	1.48	23.1	197	2E28
B0412-204	2.51	1	G	0.69	12.7	90	5E27
B0413-210	7.3	0.73	Q	1.63	5	43	1E29
B0413-296	3.71	1.07	Q	0.807	39	294	1E28
B0415-221	1.4	0.77	G		14.6		

Table 2 – *continued*

Source Name (1)	S_{408} Jy (2)	α (3)	Opt Obj (4)	z (5)	θ " (6)	l kpc (7)	P_{408} W Hz ⁻¹ (8)
B0418-288	1.16	0.96	Q	0.85	1.99	15	4E27
B0420-263	2.82	0.7	G	0.131	219	506	7E29
B0421-225	1.72	0.78	Q	0.364	8.1	41	7E26
B0422-249	1.41	0.77	G		4.9		
B0424-268	3.25	0.87	G	0.47	22.5	132	3E27
B0428-236	1.12	0.76	U		8.9		
B0428-271	1.72	0.83	G	0.84	46.4	355	5E27
B0428-281	2.49	0.89	G	0.65	61.9	429	4E27
B0429-267	1.32	1.11	G	1.27	6.9	58	1E28
B0430-235	0.96	0.86	G	0.82	91	691	3E27
B0430-278	0.95	0.76	Q	1.63	1.99	17	1E28
B0431-250	1.01	1.25	U		16.4		
B0431-292	1.67	1.57	G	0.406	1.2	6	1E27
B0436-203	0.97	0.53	U		3.5		
B0436-294	1.2	0.99	G	0.808	13.5	102	4E27
B0437-244	1.28	0.93	Q	0.84	126	964	4E27
B0437-253	1.26	0.75	G		20.2		
B0442-282	18.85	0.97	G	0.147	85.6	218	1E27
B0442-285	1.33	1.16	G		1.4		
B0442-289	3.27	1.11	U		11.9		
B0445-221	4.64	0.89	G		1.9		
B0447-230	0.96	0.83	Q	2.14	1.99	17	3E28
B0450-221	3.23	1.11	Q	0.898	14.3	112	1E28
B0450-288	1.44	0.94	G		13.2		
B0454-220	4.93	0.78	Q	0.533	84	529	5E27
B0457-235	1.12	1.13	G	1.96	16.6	141	4E28
B0457-247	1.25	0.7	G	0.186	60	185	1E26
B0458-208	0.95	1.1	G		33.8		
B0508-220	5.1	0.81	G	0.16	38.5	105	3E26
B0516-275	1.37	0.81	G		1.9		

Table 2 – *continued*

Source Name (1)	S_{408} Jy (2)	α (3)	Opt Obj (4)	z (5)	θ " (6)	l kpc (7)	P_{408} W Hz ⁻¹ (8)
B0519-208	7.34	1.18	G		1.6		
B0522-215	1.75	1	Q	1.83	2.5	21	4E28
B0522-239	1.08	0.8	G	0.5	23.4	142	9E26
B0522-263	1.36	0.91	G	0.29	4.9	21	3E26
B0524-234	1.26	0.87	G		5.7		
B0527-255	1.54	0.88	G		2		
B0528-212	2.39	1.08	G		34.5		
B0529-210	1.33	0.96	G	0.42	40	220	8E26
B0541-243	3.61	0.98	G	0.523	20	125	4E27
B0541-288	0.99	0.79	G		1.9		
B0543-265	2.63	0.88	G	0.85	23.9	184	9E27
B0549-213	1.7	0.83	Q	2.245	3.6	30	5E28
B0551-226	1	0.71	G		70.5		
B0552-249	1.31	0.86	G		4.3		
B0555-229	0.95	0.89	G		10.2		
B0556-281	2.26	1.04	G		6.8		
B0556-289	2.39	0.59	G		3.5		
B0557-235	1.14	0.96	G		21.2		
B0600-219	1.04	1.09	G	1.71	4.2	36	2E28
B0602-289	1.37	1.03	G	0.56	37	239	2E27
B0614-295	1.04	0.81	G		9.1		
B0930-200	3.26	1	G	0.769	20.2	150	9E27
B0937-250	1.37	1.07	G		66.3		
B0938-205	1.35	0.88	G	0.371	69.4	354	6E26
B0941-200	1.03	0.88	Q	0.715	47.7	344	2E27
B0943-242	1.05	1.23	G	2.93	3.5	28	1E29
B0946-237	1.19	0.77	G		7.8		
B0946-262	1.74	1.02	G		40.8		
B0947-217	1	1.01	U		24.2		
B0947-249	4.98	1.07	G	0.854	69.1	532	2E28

Table 2 – *continued*

Source Name (1)	S_{408} Jy (2)	α (3)	Opt Obj (4)	z (5)	θ " (6)	l kpc (7)	P_{408} W Hz ⁻¹ (8)
B0949-206	1.91	0.95	G	1.158	6	50	1E28
B0950-239	1.38	0.75	G		19		
B0952-224	1.71	0.62	G	0.228	6.2	22	2E26
B0955-283	1.43	0.91	G		77.7		
B0955-288	3.7	1	G	1.406	4.9	42	5E28
B0956-256	2.21	0.94	G		1.9		
B0958-227	1.02	0.58	G	0.7	1.9	14	2E27
B0959-225	1.04	0.68	G	0.895	11.3	88	3E27
B0959-236	1.15	0.54	G		41.4		
B0959-263	1.72	0.82	G	0.677	39.3	277	3E27
B1002-215	6.71	1.46	G	0.59	29.1	193	1E28
B1002-216	2.11	0.65	G	0.49	1.9	11	2E27
B1006-214	1.35	0.78	G	0.246	191	732	2E26
B1006-286	3.54	0.76	G	0.582	10.2	67	4E27
B1006-299	1.44	0.94	Q	1.064	18.3	149	8E27
B1008-233	1.56	0.62	G	1.18	1.9	16	9E27
B1009-259	1.75	0.76	G		15		
B1010-271	1.42	1.09	Q	0.436	44.3	250	1E27
B1011-282	2.6	1.04	Q	0.255	64	252	5E26
B1012-237	2.09	1.02	G	0.993	33.1	266	1E28
B1014-200	1.52	0.71	G		1.9		
B1014-278	1.5	0.92	U		3.4		
B1017-220	1.04	0.58	G	1.768	1.9	16	1E28
B1019-227	0.96	0.98	Q	1.55	2.2	19	1E28
B1021-217	1.18	1.06	G		4		
B1022-241	1.04	0.8	G		27.6		
B1022-250	0.99	0.84	G	0.34	51.6	249	4E26
B1022-299	1.12	0.84	G	0.911	2	16	4E27
B1023-226	1.08	0.94	G	0.586	58.6	387	1E27
B1023-243	1.21	0.92	G		6.1		

Table 2 – *continued*

Source Name (1)	S_{408} Jy (2)	α (3)	Opt Obj (4)	z (5)	θ " (6)	l kpc (7)	P_{408} W Hz ⁻¹ (8)
B1025-229	1.05	1.17	Q	0.309	188	849	3E26
B1025-264	1.53	0.63	Q	2.665	10.2	82	6E28
B1025-270	1.82	0.83	G	0.72	12.8	93	4E27
B1025-293	1.46	0.96	G		22		
B1026-202	1.95	0.88	G	0.566	62.1	403	2E27
B1027-225	1.11	1.1	G	0.15	47	122	7E25
B1029-233	1.08	0.86	G	0.611	72	485	2E27
B1033-251	1.53	0.83	G	0.44	84.3	478	1E27
B1033-259	1.05	0.66	G		0.9		
B1034-265	1.37	0.92	U		3.8		
B1035-288	1.77	0.84	G	1.276	7.9	67	1E28
B1036-215	0.98	0.82	G	0.585	41	271	1E27
B1040-285	1.09	0.99	G	1.63	6.4	55	2E28
B1043-216	1.83	1.13	G	1.105	3.1	26	1E28
B1048-211	1.5	1.07	U		1.9		
B1048-238	1.31	0.76	G	0.206	82	275	2E26
B1048-272	2.41	0.79	G	1.558	1.9	16	3E28
B1049-201	4.46	0.98	G	1.116	4.4	36	3E28
B1051-274	0.97	1.13	G		38.8		
B1052-272	2.05	1.07	Q	1.103	76.5	630	1E28
B1055-242	1.95	0.51	Q	1.09			9E27
B1056-272	0.97	0.97	G	0.25	7.1	28	2E26
B1103-208	7.64	0.99	G	1.12	9.7	80	5E28
B1106-227	1.81	0.73	Q	1.875	0.99	8	3E28
B1106-258	0.97	1.26	G	2.43	3.6	30	6E28
B1107-218	1.04	0.95	G		53.8		
B1107-227	2.89	1.12	G		68.5		
B1107-272	1	0.97	U		6.8		
B1108-212	1.01	0.84	G		13.9		
B1110-217	2.69	0.54	G		1.9		

Table 2 – *continued*

Source Name (1)	S_{408} Jy (2)	α (3)	Opt Obj (4)	z (5)	θ " (6)	l kpc (7)	P_{408} W Hz $^{-1}$ (8)
B1112-239	1.46	1.06	G	1.538	30.7	263	2E28
B1114-217	1.32	0.94	G		13.6		
B1114-220	1.61	0.72	Q	2.282	0.99	8	5E28
B1117-217	1	1.08	G		36.4		
B1117-248	2.69	0.54	Q	0.462			2E27
B1121-238	1.57	1.09	Q	0.675	46	324	3E27
B1126-246	1.1	0.74	G	0.155	51.7	138	7E25
B1126-258	1.13	1.01	G	0.979	8.1	65	6E27
B1126-290	2.42	0.74	G	0.41	105	570	1E27
B1128-268	1.09	1.05	G	1.43	7	60	1E28
B1129-250	0.98	0.91	G	1.065	32	261	6E27
B1131-269	2.36	1.32	G	1.711	0.9	8	7E28
B1132-258	2.56	0.88	U		0.9		
B1136-211	1.1	1.02	G	0.87	25.5	197	4E27
B1137-257	0.95	0.62	G		2.9		
B1138-262	4.12	1.34	G	2.17	11.1	93	2E29
B1139-285	6.81	0.85	G	0.85	13	100	2E28
B1142-206	1.42	1.03	G		54.5		
B1142-242	1.15	0.9	G		13.6		
B1145-248	1.04	0.76	G		17.4		
B1151-298	1.44	0.85	Q	1.376	4	34	1E28
B1152-204	0.98	0.81	G		13.7		
B1153-231	1.94	0.94	G		45		
B1155-214	1.27	0.95	G		32		
B1156-221	2.66	0.61	Q	0.563			3E27
B1158-275	0.98	0.9	G		9.5		
B1202-262	3.55	0.53	Q	0.786	15	112	8E27
B1208-277	1.58	0.83	Q	0.828	43.4	331	5E27
B1210-290	1.08	0.89	G		6		
B1211-259	1.1	0.83	G		8.4		

Table 2 – *continued*

Source Name (1)	S_{408} Jy (2)	α (3)	Opt Obj (4)	z (5)	θ " (6)	l kpc (7)	P_{408} W Hz ⁻¹ (8)
B1211-272	0.97	0.98	G	1.893	2.6	22	2E28
B1212-204	1.32	0.94	G		42		
B1212-275	0.96	0.96	Q	1.656	3.5	30	2E28
B1217-209	1	0.94	Q	0.814	29.8	226	3E27
B1217-276	1.03	1.19	G	1.899	7.5	64	3E28
B1219-264	1.13	1.22	G		93		
B1222-293	1.33	0.76	Q	0.816	29.4	223	4E27
B1224-208	1	1.09	G		62		
B1224-262	3.18	0.83	Q	0.768	1.99	15	8E27
B1226-211	3.28	0.8	G	0.191	29.3	92	3E26
B1226-297	1.2	0.84	Q	0.749	64.5	474	3E27
B1230-244	1.93	0.93	G	0.257	3.4	13	4E26
B1232-249	5.1	0.83	Q	0.352	109	537	2E27
B1235-226	1.92	0.89	G	0.778	7.1	53	5E27
B1236-200	1.04	0.96	G		3		
B1238-236	1.11	0.93	G	0.9	5.9	46	4E27
B1239-256	0.96	1.01	G		12.8		
B1240-209	4.58	0.87	G	0.42	18.8	104	3E27
B1240-271	1.45	1.01	G		1.9		
B1241-275	1.67	1.33	G		17		
B1241-291	1.37	1.1	G		17.6		
B1245-292	1.81	1	G		21		
B1246-206	1.18	0.78	G		46.2		
B1246-231	1.17	0.63	G	0.68	1.9	13	2E27
B1247-290	1.87	0.91	Q	0.77	57.6	428	5E27
B1254-268	1.14	0.74	G	0.135	24.5	58	5E25
B1255-282	1.15	0.93	G		39.1		
B1257-230	3.23	1.05	Q	1.109	52	428	2E28
B1258-211	1.52	1.19	G	1.58	2.6	22	3E28
B1259-200	3.57	1.15	G	1.58	9.9	85	7E28

Table 2 – *continued*

Source Name (1)	S_{408} Jy (2)	α (3)	Opt Obj (4)	z (5)	θ " (6)	l kpc (7)	P_{408} W Hz $^{-1}$ (8)
B1301-251	1.16	0.79	Q	0.952	8.7	69	5E27
B1302-206	1.2	1.06	G		18.2		
B1303-215	1.46	0.76	G	0.12	70	150	5E25
B1303-250	1.51	0.8	Q	0.738	38.5	281	3E27
B1306-262	1.19	0.86	G		56		
B1307-217	1.09	0.92	G		14		
B1308-220	22.21	1.19	G	0.8	1.1	8	7E28
B1309-201	1.79	0.82	G		1.9		
B1309-211	1.67	0.83	G	0.3	53.7	238	5E26
B1309-216	1.03	0.69	Q	1.49	3	26	1E28
B1309-294	1.22	0.82	G	0.67	3.2	22	2E27
B1311-270	1.77	0.82	Q	2.186	19.5	164	5E28
B1312-274	1.78	1.17	G		32.4		
B1313-248	2.14	0.9	G	0.74	27.7	203	5E27
B1313-267	1.05	1.01	U		13.5		
B1324-262	1.39	1.1	G	2.28	1.6	13	6E28
B1325-222	2.12	0.99	G	0.4	3.8	20	1E27
B1325-257	1.16	0.93	G	0.62	45.4	308	2E27
B1327-214	5.63	0.82	Q	0.528	31	194	6E27
B1328-257	4.8	1.03	G		5		
B1329-257	3.73	0.89	G	0.19	48.8	153	4E26
B1331-214	1.05	0.97	G		22		
B1336-276	1.03	1.05	G		3.5		
B1344-216	2.7	0.87	G	0.33	1.9	9	9E26
B1346-252	1.27	1.26	G	0.125	55	122	5E25
B1349-265	3.59	0.63	Q	0.934	1.99	16	1E28
B1351-211	2.29	0.94	Q	1.262	11	93	2E28
B1351-235	1.77	1.11	U		10.6		
B1353-216	1.44	1.13	G		23		
B1353-245	1.38	0.96	G		3.4		

Table 2 – *continued*

Source Name (1)	S_{408} Jy (2)	α (3)	Opt Obj (4)	z (5)	θ " (6)	l kpc (7)	P_{408} W Hz ⁻¹ (8)
B1355-215	1.87	0.8	Q	0.832	4.2	32	6E27
B1355-236	1.44	0.95	Q	1.604	16	137	2E28
B1357-217	0.96	0.96	G		15.2		
B1358-214	1.48	1.08	G	0.5	90	548	1E27
B1359-281	2.3	0.52	Q	0.802	1.4	11	5E27
B1401-296	3.28	0.83	G		12.7		
B1402-253	2.37	0.98	G	0.74	5	37	6E27
B2021-208	1.65	1.16	Q	1.2	24.5	205	2E28
B2024-217	2.45	0.88	Q	0.459	31	180	2E27
B2025-206	1.94	1.12	Q	1.4	32.5	277	3E28
B2025-218	1.28	1.07	G	2.63	4	32	8E28
B2028-223	2.58		U				
B2028-293	1.38	0.99	G	0.498	4.9	30	1E27
B2030-230	6.45	1	Q	0.132	70	163	3E26
B2035-203	1.87	0.77	Q	0.516	64	396	2E27
B2036-254	1.19	1.06	G	2	5.9	50	4E28
B2037-234	0.96	0.93	Q	1.15	15	124	7E27
B2038-280	1.47	1.23	G	0.39	150	790	8E26
B2039-236	1.63	0.86	G	0.621	45	305	2E27
B2039-291	3.02	0.91	G		15.1		
B2040-219	1.2	1.08	G	0.204	7.1	24	1E26
B2040-236	1.05	0.61	Q	0.704	56	401	2E27
B2042-293	1.18	0.92	G		65		
B2044-272	1.12	0.89	U		0.9		
B2045-245	1.99	1	G	0.73	77	560	5E27
B2045-256	3.08	1.21	G		0.9		
B2045-260	0.95	1.12	G		25		
B2048-272	1.98	1.27	G	2.06	5.3	45	9E28
B2052-253	1.09	1.23	G	2.6	18.1	147	8E28
B2053-201	6.37	0.8	G	0.155	29.7	79	4E26

Table 2 – *continued*

Source Name (1)	S_{408} Jy (2)	α (3)	Opt Obj (4)	z (5)	θ " (6)	l kpc (7)	P_{408} W Hz ⁻¹ (8)
B2057-286	2.34	0.93	G	0.605	12.3	82	3E27
B2058-237	1.47	0.96	G		1.9		
B2059-228	1.41	0.93	G		28.4		
B2100-280	2.37	0.79	G		12.5		
B2101-214	0.96	0.73	G	0.198	31.9	104	1E26
B2104-242	1.8	1.35	G	2.49	21.8	179	1E29
B2104-256	28.1	0.79	G	0.037	270	196	9E25
B2104-290	0.97	1	G		21.6		
B2105-238	1.47	1.03	G		33		
B2107-285	1.53	0.66	G		43.8		
B2111-259	5.27	0.91	Q	0.602	9	60	8E27
B2111-275	0.95	1.38	G		19		
B2113-211	9.05	0.96	G	0.698	40.4	289	2E28
B2115-253	1.23	1.19	G	1.114	1.7	14	1E28
B2116-250	1.74	0.89	G	0.467	46	270	1E27
B2116-294	1.01	0.88	U		77		
B2117-269	2.6	0.77	G	0.103	31.3	59	7E25
B2118-266	1.17	0.58	G	0.343	80	388	4E26
B2118-296	0.97	1.18	G		8		
B2122-238	1.05	0.71	Q	1.774	1.6	14	2E28
B2123-292	2.12	0.99	G		24.2		
B2125-237	2.21	1.09	G	0.95	1.9	15	1E28
B2126-230	2.58	1.05	G		35		
B2128-208	6.15	0.97	Q	1.62	1.99	17	1E29
B2131-241	1.04	0.92	G		1.9		
B2132-236	0.95	0.95	G	0.81	54.5	412	3E27
B2135-209	9.76	0.79	G	0.635	1.9	13	1E28
B2135-257	1.38	0.9	G	1.31	1.9	16	1E28
B2136-251	1.2	0.57	Q	0.94	1.99	16	4E27
B2136-261	2.93	1.01	G		29.8		

Table 2 – *continued*

Source Name (1)	S_{408} Jy (2)	α (3)	Opt Obj (4)	z (5)	θ " (6)	l kpc (7)	P_{408} W Hz ⁻¹ (8)
B2137-279	1.21	0.94	G	0.64	59.2	407	2E27
B2139-292	1.66	1.09	G	2.55	6.8	56	1E29
B2144-236	1.34	1.12	G		13.2		
B2144-279	1.09	0.83	G		37.8		
B2148-228	1.42	0.99	G	0.85	21	161	5E27
B2149-200	5.12	0.9	Q	0.424	2	11	3E27
B2149-287	5.68	0.64	G	0.479	1.9	11	4E27
B2150-202	2.68	1.2	G		39.4		
B2151-283	1.49	1.24	U		10.4		
B2154-293	1.01	0.86	G	0.63	1.9	13	2E27
B2155-255	0.98	1.48	G		2.7		
B2156-245	1.39	0.87	Q	0.862	1.99	15	5E27
B2158-206	1.15	0.87	Q	2.272	0.99	8	4E28
B2159-201	1.74	1.27	G		2.7		
B2200-251	1.27	1	G		11.3		
B2201-272	1.47	0.9	G	0.93	5.8	46	6E27
B2204-202	2.9	1.18	G	1.61	2	17	6E28
B2206-237	3.78	0.51	G	0.087	1.9	3	7E25
B2206-251	2.04	0.93	G	0.158	104	281	1E26
B2210-283	1.42	0.64	G		1.9		
B2211-252	1.25	0.94	G		17.7		
B2211-251	2.3	0.98	Q	2.508	2.4	20	1E29
B2213-283	2.54	0.98	Q	0.946	58	460	1E28
B2216-206	1.23	1.03	G	1.148	88.6	735	9E27
B2216-281	6.24	1.03	G	0.657	1.9	13	1E28
B2217-251	2.45	1.07	G		1.9		
B2222-277	1.36	0.82	G		8.4		
B2224-273	1.15	1.32	G	1.68	0.9	8	3E28
B2226-224	1.25	0.89	G	0.38	10.4	54	6E26
B2226-297	1.2	1	G	0.73	4.9	36	3E27

Table 2 – *continued*

Source Name (1)	S_{408} Jy (2)	α (3)	Opt Obj (4)	z (5)	θ " (6)	l kpc (7)	P_{408} W Hz ⁻¹ (8)
B2227-214	1.81	1	Q	1.41	15.1	129	2E28
B2229-228	1.1	0.86	G	0.542	6.6	42	1E27
B2230-206	1.01	0.66	G	0.6	5.8	39	1E27
B2232-232	2.19	0.79	G	0.87	15	116	7E27
B2232-272	1.11	0.89	Q	1.495	16	137	1E28
B2236-264	1.23	0.83	G	0.43	25.7	144	8E26
B2238-216	1.07	1	G	0.401	7.1	38	6E26
B2247-232	3.3	1.02	G	1.33	9.3	79	4E28
B2247-248	1.05	0.9	G	1.63	13.1	112	2E28
B2248-223	1.3	0.89	G	0.307	71	319	4E26
B2250-210	1.11	0.85	G	0.72	2.9	21	2E27
B2254-248	1.81	0.68	G	0.54	25	159	2E27
B2255-228	1.12	1.35	G		0.9		
B2256-207	1.21	1.02	G	0.87	32.7	253	5E27
B2256-217	1.33	1.23	Q	1.779	33.2	284	4E28
B2257-270	1.45	0.62	Q	1.476	0.99	8	1E28
B2303-253	2.52	1.07	G	0.73	18.6	135	6E27
B2304-257	1.27	0.94	G		1.2		
B2307-282	3.1	1	G		37.6		
B2308-214	0.99	0.83	G	0.151	58.5	152	6E25
B2311-222	2.24	0.78	G	0.434	80	450	1E27
B2313-277	1.9	0.97	G	0.614	44.2	298	3E27
B2314-211	1.15	1.08	G		17		
B2317-223	1.793	1.24	G		34.9		
B2317-277	5.44	0.73	G	0.173	210	612	4E26
B2318-244	2.42	0.93	G	1.12	25	206	2E28
B2320-269	0.97	0.9	G	0.99	1.9	15	5E27
B2322-275	3.07	0.72	G	1.27	22.3	188	2E28
B2324-259	1.44	0.72	G	0.286	21.7	93	3E26
B2325-213	3.07	0.94	G	0.58	79	519	4E27

Table 2 – *continued*

Source Name (1)	S_{408} Jy (2)	α (3)	Opt Obj (4)	z (5)	θ " (6)	l kpc (7)	P_{408} W Hz ⁻¹ (8)
B2326-254	1.91	0.98	G		2.4		
B2327-215	2.05	0.88	G	0.28	4.9	21	5E26
B2329-251	2.75	1.12	G		18.4		
B2338-233	1	0.82	Q	0.715	29.5	213	2E27
B2338-290	1.28	0.75	Q	0.446	73	417	8E26
B2340-219	2.35	1.06	G	0.766	27.1	201	7E27
B2341-244	1.55	0.74	G	0.59	2.1	14	2E27
B2343-243	1.85	0.8	G	0.6	48.3	323	2E27
B2348-235	1.47	0.83	G	0.952	68.7	546	6E27
B2348-252	4.41	1.13	Q	1.386	33.5	285	6E28
B2351-222	1.41	1	G		24.1		
B2351-234	1.61	0.92	G	1.03	28.8	234	9E27
B2355-214	2.09	1.23	G	1.41	2.8	24	3E28
B2359-259	1.02	0.81	G		1.9		